



Development and numerical investigation of new non-linear Kalman filter variants

A.C. Charalampidis G.P. Papavassilopoulos

School of Electrical and Computer Engineering, National Technical University of Athens, Athens, Greece
 E-mail: alexcharal@yahoo.gr

Abstract: This study deals with recursive state estimation for non-linear systems. A new set of σ -points for the unscented Kalman filter is proposed as well as a way to substitute a non-linear output with a linear one. The importance of the function of the state which must be estimated is also illustrated and also the need for taking it into account when designing the state estimator. Mode-based estimators are proposed. All the suggested methods are compared with standard extended Kalman filter, unscented Kalman filter and particle filter with sampling importance resampling using simulations. The results show that the modifications proposed in some cases lead to considerable reduction in the estimation error.

1 Introduction

Estimating the state of a dynamical system is a common task. In practice, all measurements are noisy and all processes are affected by some kind of disturbance. For linear equations with normally distributed disturbance and measurement error stochastic processes, it is well known that the Kalman filter (KF) [1] provides an exact solution of the problem. The problem can be also solved exactly if the state space is finite.

In this paper non-linear discrete time systems with additive noise are considered. For these systems, even if all disturbances are normally distributed, the non-linearities distort the distribution, thus leading to non-normal distributions for the state of the system. For low-dimensional systems, it is feasible to approximate the exact state distribution by partitioning the state space. Other approximate solutions, which do not suffer from the curse of dimensionality, are provided by the extended Kalman filter (EKF) [2], the unscented Kalman filter (UKF) (see [3]) and various forms of particle filters (PFs) (see [4, 5]). These filters are discussed briefly in the next section. Reference [6] provides a comparison of different variants of KF-based non-linear filters.

For the UKF, the selection of σ -points is an important issue. Several aspects of this selection are treated in [3]. A new selection algorithm is presented in this paper, and in some cases it outperforms significantly the standard algorithm of [7].

Apart from the system dynamics, non-linearities may be present in the output equations. Under certain conditions, inverting the non-linearity and assuming a linear output equation can help to avoid non-linear overshoot-like phenomena. This is illustrated with an appropriate example, and it is shown using simulations that by this way the error of the EKF can be reduced significantly. The use of

mode-based filters can also reduce the estimation error under the presence of strong non-linearities in the output equations.

The quantity that must be estimated is also shown to be very important for the correct selection of the filtering algorithm. Except for the fact that different standard filters may estimate better different system states or different system state functions, it is possible, in some cases, to design filters specifically for the estimation of some function of the state. This is presented through a suitable example in Section 3.2.

The remainder of this paper is organised as follows. In Section 2 the problem formulation and some basic results are presented. The standard filtering techniques to be compared with the proposed ones are also presented. In Section 3 the proposed modifications are described. Section 4 presents simulation examples used to compare the performance of the techniques under consideration. Conclusions are drawn in Section 5.

2 Background

2.1 Problem formulation

The dynamical systems considered are described by equations of the form

$$x_{k+1} = f(x_k) + w_k \quad (1)$$

$$y_k = h(x_k) + v_k \quad (2)$$

where $x_k \in \mathbb{R}^n$ is the state of the system and $y_k \in \mathbb{R}^m$ is the measured output at time k . w_k is the disturbance, also referred to as process noise, and v_k is the measurement noise. In this paper only i.i.d. noise sequences will be considered. The initial condition is x_0 is independent of

the noise sequences and follows a known distribution. Measurements are available from time $k = 1$ onwards.

The problem is to estimate a function of the state, $z_k = g(x_k)$. The function g can be the identity, the output function h or another function. Since z_k will be a random variable, it may be desired to approximate its probability density function (pdf) or only some statistics of it, such as the expected value or the covariance. As will be made apparent, the choice of g and of the statistics that must be estimated has a heavy impact on the whole procedure.

Suppose now that $p_{x0}(x_0)$ is the pdf of x_0 , $p_V(v_k)$ is the pdf of the measurement noise and $p_W(w_k)$ is the pdf of the process noise. It holds $p_{Y|X}(y_k|x_k) = p_V(y_k - h(x_k))$ and $p_{X_{k+1}|X_k}(x_{k+1}|x_k) = p_W(x_{k+1} - f(x_k))$. The subscripts of pdfs will be omitted for convenience. Let us define $y_{1:k} = \{y_1, y_2, \dots, y_k\}$.

Then, using Bayes rule [8, 9], the following recursive equations (see, e.g. [4, 9]) hold

$$p(x_{k+1}|y_{1:k}) = \int p(x_{k+1}|x_k)p(x_k|y_{1:k}) dx_k \quad (3)$$

$$p(x_{k+1}|y_{1:k+1}) = p(y_{k+1}|x_{k+1})p(x_{k+1}|y_{1:k})/c_k \quad (4)$$

where

$$c_k = \int p(y_{k+1}|x_{k+1})p(x_{k+1}|y_{1:k}) dx_{k+1} \quad (5)$$

However, except for some special cases, the above integrals cannot be evaluated analytically. Numerical integration for a sufficiently dense mesh of x_k at each time step is also impractical, so (3)–(5) are mainly of theoretical interest.

2.2 Standard filtering techniques

In EKF the system (1) and (2) are linearised and then KF equations are used. Specifically, if \hat{x}_k is the estimated mean of x_k after the correction step of time k and \hat{x}_{k+1}^- is the estimated mean of x_{k+1} after the prediction step of time $k + 1$, then for the prediction step the function f in (1) is linearised around \hat{x}_k , while for the correction step the function h in (2) is linearised around \hat{x}_{k+1}^- . The covariance matrices and the correction gain are then calculated using KF equations. As is obvious, it is assumed that the derivatives of f and h are available.

The intuition behind UKF is that ‘it is easier to approximate a probability distribution than it is to approximate a non-linear function or transformation’ [7]. Thus, the system equations are not simplified but the prior distribution is approximated by a finite sum of Dirac deltas. The procedure which follows applies to systems with additive noise. For the general case as well as for justification and criteria for parameter choice, refer to [3, 7]. In this paper, the UKF will be applied with the choice of parameters (see below) $\alpha = 1$, $\beta = 2$, $\kappa = 3 - n_x$, where n_x is the dimension of the state space.

Suppose that after time k the estimated covariance of the state is P_{x_k} . Then $2n_x + 1$ σ -points are calculated: $X_{0,k} = \hat{x}_k$, $X_{i,k} = \hat{x}_k + \gamma S_i$, $i = 1, \dots, n_x$ and $X_{i,k} = \hat{x}_k - \gamma S_i$, $i = n_x + 1, \dots, 2n_x$, where S_i is the i th column of the matrix S provided by the Cholesky decomposition of P_k (namely S is such that $P_k = SS^T$) while $\gamma = \sqrt{n_x + \lambda}$, $\lambda = \alpha^2(n_x + \kappa) - n_x$, α and κ being parameters.

For the prediction step, the σ -points are transformed through $x_{k+1} = f(x_k)$ and thus the covariance and mean before the correction can be calculated. Of course, the covariance of w_k is added to the covariance of the transformed σ -points to yield the prediction covariance. The weights used for the mean and covariance calculations are

$$W_m^{(0)} = \frac{\lambda}{n_x + \lambda}, W_c^{(0)} = \frac{\lambda}{n_x + \lambda} + 1 - \alpha^2 + \beta \quad (6)$$

$$W_m^{(i)} = W_c^{(i)} = \frac{1}{2(n_x + \lambda)} \quad (7)$$

where β is also a parameter.

For the correction step, with the new mean and covariance, $2n_x + 1$ σ -points $X_{i,k+1}^-$, $i = 0, \dots, 2n_x$ are analogously calculated. These are transformed through $y_{k+1} = h(x_{k+1})$ and thus the mean and covariance of the measurement vector can be calculated (to obtain the covariance of y_k , the covariance of v_k is added to the calculated covariance of the transformed σ -points), as well as the cross-covariance between the measurement and the state vector. Then the Kalman gain and the corrected estimates are computed according to the KF equations.

EKF and UKF are based on the assumption that for each time step, the state distribution can be well approximated by a normal distribution. Since in many cases this assumption does not hold, and the form of the distribution is a priori unknown, there is need for a filtering technique which permits approximation of arbitrary distributions. In PF the state pdf is approximated by a number of particles, each representing a Dirac delta with a corresponding weight, that is

$$p(x_k|y_{1:k}) \simeq \sum_{i=1}^N W_k^i \delta_{x_k^i}(x_k) \quad (8)$$

Then the mean value of a function g of the state can be estimated with the next equation.

$$\mathbb{E}[g(x_k)] \simeq \sum_{i=1}^N W_k^i g(x_k^i) \quad (9)$$

It is reasonable to conjecture that with sufficiently many particles the approximation will be good, although the asymptotic analysis of PF is a difficult problem [10, 11].

There are many different algorithms [4, 12] for the update of W_k^i and x_k^i . For the comparison purposes of this paper only sampling importance resampling (SIR) filtering, which consists the first such PF and was proposed by [13] will be used. The resampling step is implemented with stratified resampling [14]. Since the present paper does not propose any novelty on PF, no further details about PFs are presented here.

3 Proposed modifications

3.1 Inverting the output equation

Let us assume that EKF is used in the following motivating example. Suppose that the system dynamics are described by (10), where η is the disturbance.

$$\dot{x} = -\alpha x^3 + \eta \quad (10)$$

The simplest discrete time approximation with time step δ is given by the following equation, in which w_k is the effect of the disturbance.

$$x_{k+1} = x_k - \alpha\delta x_k^3 + w_k \quad (11)$$

However, $x - \alpha\delta x^3$ is not a monotonous function of x , although it should be so as to yield an acceptable approximation of the dynamics of (10). Since it has a maximum for

$$x_\infty = \frac{1}{\sqrt{3\alpha\delta}} \quad (12)$$

the following approximation captures better the dynamics of the continuous time.

$$x_{k+1} = f(x_k) + w_k, f(x) = \begin{cases} x - \alpha\delta x^3, & |x| < x_\infty \\ -\frac{2}{3}x_\infty, & x \leq -x_\infty \\ \frac{2}{3}x_\infty, & x \geq x_\infty \end{cases} \quad (13)$$

Suppose, also, that the output equation is (14).

$$y_k = x_k^3 + v_k \quad (14)$$

Therefore the EKF is applied to the system described by (13) and (14). Equation (14) has the form of (2) with $h(x) = x^3$. Suppose that for some time instant k it holds $\hat{x}_k^- = 1, P_{x_k}^- = 1, x_k = 2$ and $y_k = 8$, while the variance of v_k is equal to 1. Then since $h'(x) = 3x^2, h'(\hat{x}_k^-) = 3$ and the Kalman gain will be equal to $3/(3^2 + 1)$. Since the predicted output was equal to 1, EKF yields $\hat{x}_k = 1 + 0.3(8 - 1) = 3.1$.

The posterior value for the output is then greater than the observed; however, this is not due to measurement error and the predicted value was less than the observed. This happens because the first-order approximation of h obtained with its derivative is valid only locally. Thus because of the non-linearity of the output function, the filter although supposed to smooth the observed data, suffers from this overshoot-like phenomenon.

A remedy to this problem is to invert the output equation. If there were no measurement error, one would set $x_k = \sqrt[3]{y_k}$, where the cubic root of a negative number is defined appropriately. Now it holds $x_k = \sqrt[3]{y_k + v_k}$. Since v_k is a random variable, $\sqrt[3]{y_k + v_k}$ is also a random variable. It is not computationally demanding to calculate its mean and variance.

For this purpose, a suitable set $\{V_1, V_2, \dots, V_N\}$ whose distribution approximates the distribution of v_k is determined. Specifically, if $F(x)$ is the cumulative distribution function of v_k , then the set $X = \{X_n = F^{-1}(1/(2N) + (n-1)/N), n = 1, \dots, N\}$ is calculated, and then it is normalised to give the set $V = \{V_n = \sqrt{(R/\sum_{l=1}^N X_l^2)}X_n, n = 1, \dots, N\}$, where R is the variance of v_k . Then, for each step, the mean s_k and variance I_k of the set $\{\sqrt[3]{y_k + V_1}, \dots, \sqrt[3]{y_k + V_N}\}$ are calculated.

The proposed technique is to apply EKF to the system whose dynamics is given by (13) and its output equation is

$$s_k = x_k + r_k \quad (15)$$

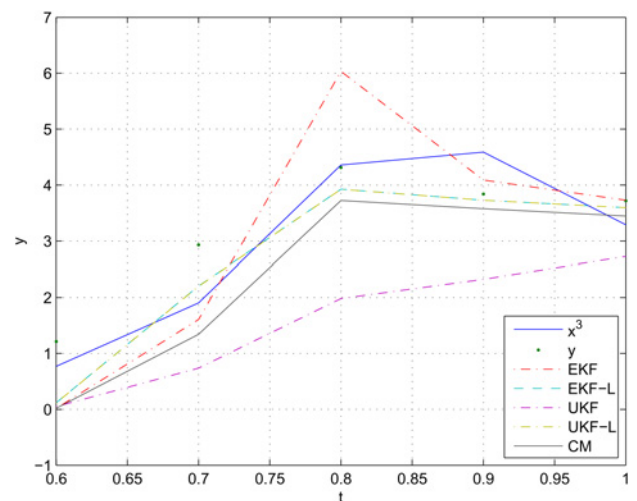


Fig. 1 Time series of output data and various estimation methods illustrating the overshoot-like phenomenon for EKF

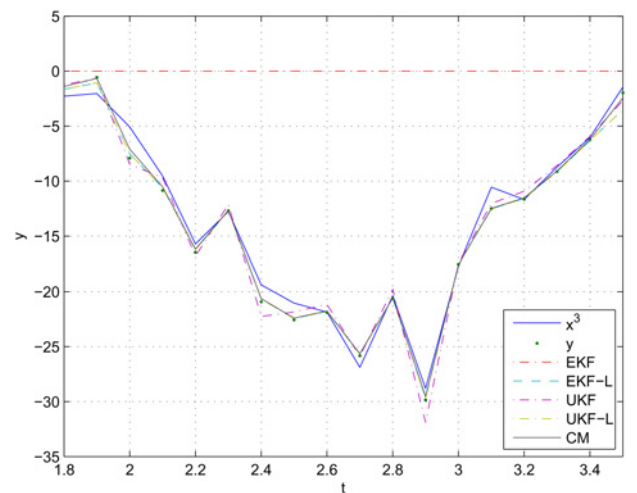


Fig. 2 Time series of output data and various estimation methods illustrating the overshoot-like phenomenon for UKF and the possibility of EKF being trapped to zero

where the variance of r_k is equal to I_k , which is obtained, together with s_k , from the inversion step.

Output inversion can also be applied to UKF. Its effectiveness is illustrated in Fig. 1, where the suffix-L implies that output inversion has been applied. Fig. 1 shows that output inversion extinguishes the overshoot phenomenon for EKF and that it is effective for UKF, too. The black curve corresponds to the expected value obtained by partitioning the state space using a constant mesh (CM) (see Section 4). In another realisation of the experiment, presented in Fig. 2, EKF is trapped to zero while UKF suffers from overshoot. Again, output inversion is effective for both EKF and UKF. Numerical values of the prediction error for all the filtering techniques tested are presented in Section 4.

3.2 Estimating a specific function of the state

Let us consider the system with system (13) and the following output equation

$$y_k = x_k^2 + v_k \quad (16)$$

Suppose that w_k and v_k are i.i.d. Gaussian processes with variance Q and R , respectively. Equation (16) has the form of (2) with $h(x) = x^2$. Suppose, also, it is known that $x_0 = 0$. Then $\hat{x}_1^- = 0$ and thus $h'(\hat{x}_1^-) = 0$, yielding zero Kalman gain and $\hat{x}_1 = 0$. Recursively one obtains $\hat{x}_k = 0$, whatever the output sequence is.

On the other hand, for every k the pdf of the state is even. In fact, if the output sequence is $\{y_1, y_2, \dots, y_k\}$, then for every pair of sequences $\{x_1, x_2, \dots, x_k\}$ and $\{v_1, v_2, \dots, v_k\}$ consistent with $\{y_1, y_2, \dots, y_k\}$, the pair $\{-x_1, -x_2, \dots, -x_k\}$ and $\{v_1, v_2, \dots, v_k\}$ is also consistent with the output sequence and equally probable. Marginalising over the possible $\{x_1, x_2, \dots, x_{k-1}\}$ and $\{v_1, \dots, v_{k-1}\}$ asserts that $p(x_k) = p(-x_k)$. Thus, the expected value of x_k is 0, exactly as predicted by EKF or UKF. However, the pdf for $k = 0, 1, 2, 5, 10, 50, 100$ (0 corresponds to the prior) in a random run presented in Fig. 3 is not at all close to the pdf of a normal distribution even for $k = 1$. Thus, if it is not the mean of x_k that must be estimated but another quantity, such as the mean of x_k^2 , EKF and UKF perform poorly. It is noted that even if $x_0 \neq 0$, since for some k the value of x_k will be close to 0, the same problem will arise.

An alternative way to estimate x_k^2 is as follows. Set $z_k = x_k^2$. Then if $|z_k| < (1/3\alpha\delta)$, it holds

$$\begin{aligned} z_{k+1} &= (x_k - \alpha\delta x_k^3 + w_k)^2 \\ &= x_k^2 - 2\alpha\delta x_k^4 + \alpha^2\delta^2 x_k^6 + w_k^2 + 2(x_k - \alpha\delta x_k^3)w_k \\ &= z_k - 2\alpha\delta z_k^2 + \alpha^2\delta^2 z_k^3 + w_k^2 + 2(x_k - \alpha\delta x_k^3)w_k \end{aligned} \tag{17}$$

whereas in different case, it holds

$$z_{k+1} = x_\infty^2 - 2\alpha\delta x_\infty^4 + \alpha^2\delta^2 x_\infty^6 + w_k^2 \pm 2(x_\infty - \alpha\delta x_\infty^3)w_k \tag{18}$$

where x_∞ is defined in (12). The expected value of the unknown term is $E[w_k^2 + 2(x_k - \alpha\delta x_k^3)w_k] = Q$. As for its variance, it depends on $|x_k|$. It is possible to create offline a look-up table containing the variance of the unknown term for many values of x_k and use it to find the variance at each time step. Thus, an estimate of x_k^2 is obtained by estimating

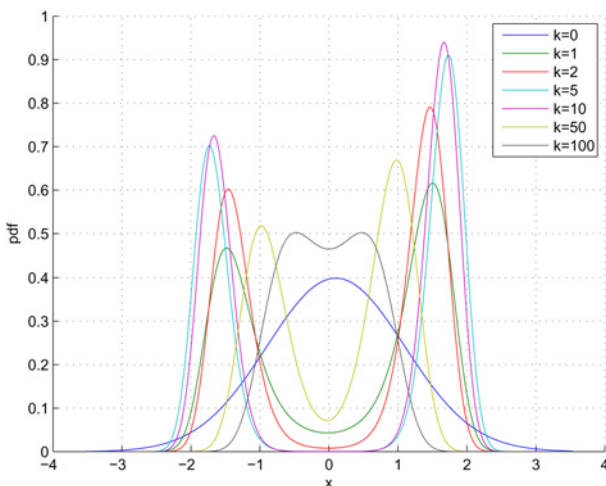


Fig. 3 Probability density function for various k in a random run

the state of the system defined by (19) and (20)

$$z_{k+1} = z_k - 2\alpha\delta z_k^2 + \alpha^2\delta^2 z_k^3 + Q + n_k \tag{19}$$

$$y_k = z_k + v_k \tag{20}$$

where n_k is zero-mean but its distribution and variance depend on z_k .

For numerical results and comparison of all the filtering techniques tested in this paper for this problem, see Section 4.2.

3.3 New σ -point set

3.3.1 One-dimensional case: The UKF algorithm of Section 2.2 approximates the normal distribution with mean M and variance P with three σ -points at $M, M - \gamma\sqrt{P}$ and $M + \gamma\sqrt{P}$, where γ as well as the corresponding weights are given in the same subsection.

More points could be used to obtain a better approximation. Let N be the desired number of σ -points. The following algorithm provides a reasonable way to approximate the normal distribution with mean M and variance P using N points. Let $\{p_i | 1/(2N) + (i-1)/N, i = 1, \dots, N\}$. Then if $F(x) = (1/\sqrt{2\pi}) \int_{-\infty}^x e^{-u^2/2} du$ is the cumulative distribution function of the standard normal distribution, calculate $\{y_i = F^{-1}(p_i), i = 1, \dots, N\}$. Then the set $\{y_i, i = 1, \dots, N\}$ is zero-mean but not necessarily of variance 1. A set of variance 1 is obtained by

$$\left\{ x_i = \sqrt{\frac{N}{\sum_{i=1}^N y_i^2}} y_i, \quad i = 1, \dots, N \right\} \tag{21}$$

The proposed σ -point set is then defined by

$$\{\sigma_i = M + \sqrt{P}x_i, \quad i = 1, \dots, N\} \tag{22}$$

and its mean and variance are equal to M and P , respectively. It is noted that both for the one-dimensional and the multi-dimensional case, the proposed points have equal weights.

3.3.2 Multi-dimensional case: Let M be the vector mean and P the covariance matrix of n -dimensional normal distribution. Since P is symmetric it is possible to find n orthonormal eigenvectors $\{v_i, i = 1, \dots, n\}$ with corresponding eigenvalues $\{\lambda_i, i = 1, \dots, n\}$. P is positive-definite, therefore all eigenvalues are positive. Let $\{z_i, i = 1, \dots, n\}$ be i.i.d. random variables following the standard normal distribution. Then the random vector $M + \sum_{i=1}^n \sqrt{\lambda_i} z_i v_i$ is normally distributed with mean M and covariance P .

Since the standard normal distribution is approximated by the set defined in (21), the following set, consisting of N^n members, can be considered as an approximation of the n -dimensional normal distribution with mean M and covariance P .

$$\left\{ \sigma_{j_1 j_2 \dots j_n} = M + \sum_{i=1}^n x_{j_i} \sqrt{\lambda_i} v_i, \quad j_i = 1, \dots, N, i = 1, \dots, n \right\} \tag{23}$$

Its mean and covariance are indeed M and P , respectively.

For large n the cardinal of the set, N^n , will be much greater than $2n + 1$ even for $N = 2$. Apart from that, the above

algorithm includes computation of the eigenvalues of P while for the set presented in Section 2.2 it is only needed to compute the square root of a positive-definite symmetric matrix, a task that can be accomplished in $O(n^3)$ time using Cholesky factorisation. However, numerical experiments with the four-dimensional example of Section 4.4 show that for that case the extra computational cost associated with the proposed σ -point set is not prohibitive.

The following example shows that the use of all combinations of j_i in $\sum_{i=1}^n x_{j_i} \sqrt{\lambda_i} v_i$ can help compute the covariance of the output much more accurately than with the σ -point set of Section 2.2. Suppose that $(x_1, x_2)^T$ is normally distributed with zero-mean and covariance matrix equal to the identity matrix, and that the mean and variance of $f(x_1, x_2) = x_1 x_2$ must be calculated. The standard algorithm uses five points, $\{(0,0), (0,1), (0,-1), (1,0), (-1,0)\}$. f maps all of them to 0, and thus the variance of f is estimated to be 0. The proposed algorithm with $N=2$ yields four points: $\{(-1,1), (1,1), (1,-1), (-1,-1)\}$. Two of them are mapped to 1 and two to -1 , thus the variance is estimated to be 1, which is the exact value. Both algorithms correctly estimate the mean to be 0.

Numerical results of the use of the proposed σ -point set in recursive state estimation are provided in the next section.

3.4 Using the mode as an approximation of the mean

KF-based non-linear filters try to approximate the mean by propagating and correcting means and covariance matrices. Except from the fact that these quantities cannot be computed exactly, the correction with the Kalman gain is not optimal for non-linear systems. On the other hand, it is possible to approximate the mode, namely the maximum of the a posteriori pdf. Although the pdf is not Gaussian, therefore the mode does not necessarily coincide with the mean, it may provide a good approximation. The calculations are made as follows.

Suppose that after the prediction step of time step k , the mean and the covariance are $\hat{x}_{k+1}^- = M$ and $P_{k+1}^- = P$, respectively. If the value of the output for time equal to $k+1$ is $y_{k+1} = y$ and the error covariance matrix is R then the pdf of x_{k+1} is equal to

$$\frac{1}{I} \frac{1}{(2\pi)^{n/2} |P|^{1/2}} e^{-(1/2)(x-M)^T P^{-1} (x-M)} \times \frac{1}{(2\pi)^{n/2} |R|^{1/2}} e^{-(1/2)(y-h(x))^T R^{-1} (y-h(x))} \quad (24)$$

where

$$I = \int \frac{1}{(2\pi)^{n/2} |P|^{1/2}} e^{-(1/2)(x-M)^T P^{-1} (x-M)} \times \frac{1}{(2\pi)^{n/2} |R|^{1/2}} e^{-(1/2)(y-h(x))^T R^{-1} (y-h(x))} dx \quad (25)$$

Thus, it is maximised for the value of x which minimises

$$\frac{1}{2} [(x-M)^T P^{-1} (x-M) + (y-h(x))^T R^{-1} (y-h(x))] \quad (26)$$

The gradient of the above expression is equal to

$$P^{-1}(x-M) + \left(\frac{\partial h(x)}{\partial x}\right)^T R^{-1}(h(x)-y) \quad (27)$$

Although the maximisation procedure described above can be used to yield an estimation of the state mean, it does not provide any estimation of the state covariance. Thus, the computed value of the covariance computed by a KF-based filter must be used for the next step. Experimentation showed that the best results are obtained by using also the computed value of the mean obtained by the KF-based filter for the next step. Thus, the values of both the mean and covariance computed by the KF-based filters are propagated between time steps, while the above procedure is performed at each time step separately to yield the mode.

4 Simulation examples

In this section the proposed filtering techniques are applied to four examples. First two one-dimensional examples are presented, then one two-dimensional example and finally one four-dimensional example of a DC motor is presented. Several variants of the KF are applied to each example, as explained in more detail in each subsection. Particle filtering with SIR is also applied for comparison purposes.

For the one-dimensional examples, the state space is partitioned with a CM and the system is approximated by a finite space Markov chain. Using this approximation, at each time step the probability that the state belongs to any mesh interval is known. The dynamics are described by a Markov matrix, which is constant and thus does not need to be calculated at each time step or at each run. The prediction step can therefore be accomplished as a multiplication of a matrix by a vector. For the correction step, the probability of each interval is multiplied by the likelihood of the observed value with respect to its centre, and then the probabilities are normalised. If the number of intervals is large enough, it is possible to obtain a good approximation not only of the state mean but also of the output mean. It must also be noted that the mesh is chosen finer near zero and coarser away from zero. On the other hand, even for the two-dimensional example, this approach would be very computationally intensive, and it has not been pursued.

It is useful to compare the results of the filters tested with the Cramer-Rao lower bound (CRLB) [15, 16]. Because the quantity (i.e. the state system) estimated is also a random variable, the Van Trees variant of the CRLB [17], also known as posterior CRLB, must be used. In [18] an efficient way to compute the posterior CLRB for the problem of discrete-time non-linear filtering is derived. More specifically, the problem described by (1) and (2) with Gaussian process and measurement noise with zero-mean and covariance matrices equal to Q and R , respectively, is treated and it is proved that it holds

$$\mathbb{E}[(\hat{x}_k - x_k)(\hat{x}_k - x_k)^T] \geq J_k^{-1} \quad (28)$$

where J_k is given by the following recursive scheme

$$J_0 = P_0^{-1} \quad (29)$$

$$J_{k+1} = D_k^{22} - D_k^{21} (J_k + D_k^{11})^{-1} D_k^{12} \quad (30)$$

$$D_k^{11} = \mathbb{E}\{[\nabla_{x_k} f^T(x_k)]Q^{-1}[\nabla_{x_k} f^T(x_k)]^T\} \quad (31)$$

$$D_k^{12} = -\mathbb{E}\{[\nabla_{x_k} f^T(x_k)]Q^{-1}\}, D_k^{21} = [D_k^{12}]^T \quad (32)$$

$$D_k^{22} = Q^{-1} + \mathbb{E}\{[\nabla_{x_{k+1}} h^T(x_{k+1})]R^{-1}[\nabla_{x_{k+1}} h^T(x_{k+1})]^T\} \quad (33)$$

where P_0 is the a priori covariance matrix of the initial state. The above formulae are valid for non-singular Q and R . For the case of singular Q or R , see the aforementioned paper.

The expected values in (31)–(33) can be approximated by computing the corresponding expressions for a large number of random runs and calculating the mean value. For the examples of this paper, 10 000 runs are made for the approximation.

It must be noted that for linear systems the bound is tight, whereas for non-linear systems the divergence between the bound and the optimal value may or may not be significant, as it will be made apparent in the following examples.

4.1 One-dimensional example with invertible output equation

In this subsection the results for the problem of estimating the state of the system with dynamics given by (13) and output given by (14) are presented. The system has been simulated under the following conditions.

- The parameters are set to $\alpha = 0.1$, $\delta = 0.1$. The initial condition x_0 is normally distributed with mean 0.1 and variance 1, and independent of w_k and v_k , which are also assumed to be normal and independent of each other. They are i.i.d. and both zero-mean.
- The variance of v_k is assumed equal to 1, while for the first case studied, the variance of w_k is equal to δ
- The system is simulated up to time $t = 10$ ($k = 100$).

To compare the different estimation methods, the experiment has been run 1000 times. The simulated mean values of x^2 and y^2 are 1.47 and 23.32, respectively. Table 1 presents the mean and the maximum (of the 1000) RMS values of the estimation error for x and y , as well as the mean computation time per step in milliseconds. All computation times in this paper have been recorded at a 64-bit PC clocked at 2.9 GHz and running MATLAB 7.2 for Linux. MATLAB is a registered trademark of The MathWorks, Inc. It must be emphasised that in this section,

by the term ‘y estimation’ estimation of $h(x)$ is meant, and similarly for the term ‘y error’. It must also be made clear that the estimated value of $h(x)$ is $h(\hat{x})$ except when it is explicitly stated that this is not the case.

EKF and UKF are the standard extended and unscented Kalman filter, respectively. MUKF stands for modified UKF. The modification implied is the use of the proposed σ -point set with $N = 9$. In the case of MUKF(P) the proposed σ -point set was used in the prediction step only. For the next three filters, the suffix ‘Mode’ denotes that the state estimate was determined by the maximisation procedure described in Section 3.4. Equation (26) is minimised by evaluating its value on a grid with step equal to 0.3, selecting the point which yields the smallest value, and then repeating using a local grid with step 0.001. This is done because experimentation showed that this is faster than iterative methods. MUKF(15) is MUKF with $N = 15$. EKF-L and UKF-L are EKF and UKF with inverted output equation, that is, with output (15) instead of (14). PF/SIR stands for particle filter with SIR, while the number in parenthesis denotes the number of particles. Since PF provides an approximation of the distribution, y can be estimated using (9). The number at the left of the slash is $\mathbb{E}[h(x_k)]$, whereas the number at the right of the slash is $h(\mathbb{E}[x_k])$ and, as expected, the former is smaller than the latter. Finally, the state space has been partitioned using a CM, as described in the beginning of this section. The number in parenthesis is the number of intervals used, while the numbers at the left and right of the slash have the same meaning as for PF, and the same comment applies to this case, too.

The results show that EKF cannot provide a satisfactory estimate for x or y . This is due to the non-linear effect described in Section 3.1. UKF is also affected by the same phenomenon, and the mean error for y is still high, although x is estimated well. MUKF and MUKF(P) are slightly better than UKF, but still unsatisfactory for y , especially MUKF which gives worse results than UKF. The mode can help in the computation of a very robust estimate of y , as is made apparent by the very low mean y -error and even better maximum y -errors, comparable only to those of CM(1000). Inverting the output equation reduces substantially the estimation error for y for both EKF and UKF, but increases the error for x . PF and CM, with many particles and intervals, respectively, perform better than UKF-L, but the fact that the y -error for EKF-L and UKF-L is smaller than that of PF(50) and CM(50) shows the

Table 1 RMS estimation error and computation time for the example of Section 4.1, case I

Estim. technique	Mean x error	Mean y error	Max. x error	Max. y error	Comp. time, ms
EKF	0.8345	18.53	3.2019	4148	0.15
UKF	0.3891	1.2593	0.6110	40.58	0.35
MUKF(P)	0.3890	1.2455	0.6050	39.22	0.60
MUKF	0.3868	1.4356	0.6577	52.40	0.75
UKF-mode	0.4117	0.7430	0.6807	1.055	0.54
MUKF-mode	0.4117	0.7449	0.6744	1.061	0.94
MUKF(15)-mode	0.4110	0.7437	0.6762	1.060	1.25
EKF-L	0.4227	0.7785	0.7237	1.263	0.71
UKF-L	0.4219	0.7775	0.7218	1.263	0.84
PF/SIR(50)	0.3872	0.8251/0.8464	0.6499	3.524/3.521	0.24
PF/SIR(1000)	0.3759	0.7212/0.7459	0.5876	1.351/1.349	1.68
CM(50)	0.3764	0.8561/0.8784	0.5882	4.434/4.438	0.07
CM(1000)	0.3753	0.7156/0.7404	0.5882	1.023/1.058	2.39

strength of the proposed technique. It is also interesting that although CM(50) yields x -error comparable to that of PF(1000), its y -error is higher than that of PF(50).

Fig. 4 presents the RMS error in the estimation of x for each time step, as well as the corresponding CRLB. The curves for 'Mode' and 'CM' are those for 'MUKF(15)-Mode' and 'CM(1000)' of Table 1. Except for the EKF, all other methods converge quickly to their steady state. It is also remarkable that the CRLB is much lower than the error of 'CM(1000)' (its RMS value is 0.1391). This happens because the non-linearities are severe, thus the bound is not tight.

Fig. 5 presents the distribution of the RMS error in the estimation of x for the same 1000 runs and for the same filters as Fig. 4. The curves for 'Mode' and 'CM' are those for 'MUKF(15)-Mode' and 'CM(1000)' of Table 1. The ineffectiveness of EKF is obvious.

The system has been also studied for variance of w_k equal to 0.1δ . For this case the simulated mean values of x^2 and y^2 are 0.58 and 2.51, respectively, while the results are presented in Table 2. Again, EKF performs poorly and UKF estimates x well, but its y -error is not satisfactory. The mode again results in an excellent y estimate, while it is also a good x estimate.

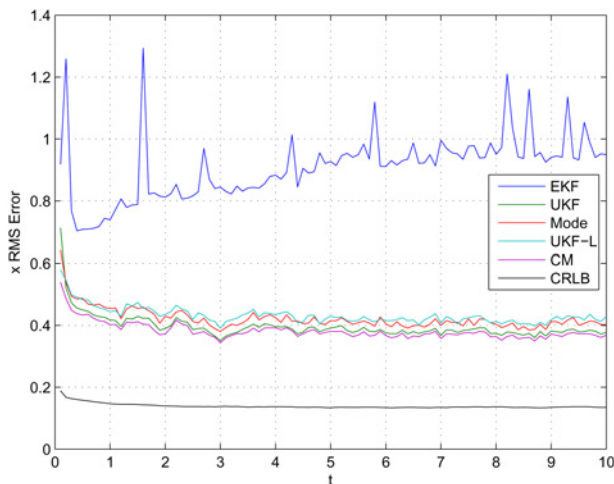


Fig. 4 Transient response of several filters and CRLB for the example of Section 4.1, case I

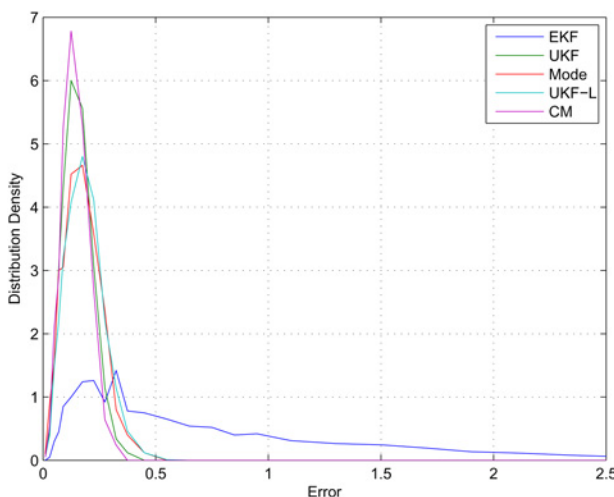


Fig. 5 RMS error distribution for the example of Section 4.1, case I

Inverting the output equation permits good estimation of y , but deteriorates the estimation of x . Finally, it can be observed that for this case CM estimates y better than PF. The RMS value of the CRLB for this case is equal to 0.1852.

4.2 One-dimensional example with non-invertible output equation

In this subsection the system with dynamics given by (13) and output given by (16) is studied. For the first case studied, the parameters as well as the distribution of x_0 are that of the preceding example. The distribution of w_k and v_k is that of the first case of that example. The system is simulated up to time $t = 10$ and 1000 runs have been made, as for the system of the previous example.

The simulated mean values of x^2 and y^2 are 1.46 and 5.82, respectively. The results are presented in Table 3. Only the estimation error for y is given, for the reasons explained in Section 4.2. The values on the second up to the fourth column correspond to the methods applied to (19) and (20) (real system), whereas those of the fifth up to the seventh column correspond to (13) and (16) (virtual system). When estimating the state of the virtual system, for simplification, n_k is assumed normally distributed. The computation times given are per step and in milliseconds.

Since the virtual system has linear output equation, output inversion is not applicable. The linearity of the output equation also implies that the mean and the mode coincide, since the distribution of the state after the prediction step is approximated by a Gaussian distribution. Thus, only the rest of the filtering techniques have been applied to this system. It must also be noted that for MUKF the modified σ -point set is applied only to the prediction step, since the output equation of the virtual system is linear and thus the update step can be accomplished using standard Kalman filtering equations.

EKF behaves well for both systems, while UKF only for the virtual one. MUKF leads to considerable error decrease in comparison with UKF only for the real system. The fact that the estimation error using EKF, UKF and MUKF for the virtual system is relatively close to that of CM or PF for the real one illustrates the efficacy of the proposed technique. Furthermore, the fact that CM(100) for the virtual system yields results comparable to those of CM(100) for the real system implies that the simplification made, that is n_k is normally distributed, does not introduce large error. This fact, in addition to the efficiency of EKF, UKF and MUKF for systems with slight non-linearities such as the virtual system, results in good performance of the aforementioned filters applied to the virtual system.

It must be noted that the computation time for CM in the case of virtual system is high because the stochastic matrix depends on the process noise variance, and thus must be calculated at each step. This is also the reason that CM(1000) has not been tested for this system.

The second case studied differs from the first one in the mean of the initial state distribution, which is 0 instead of 0.1. The simulated mean values of x^2 and y^2 for this case are 1.46 and 5.83, respectively, while the results are presented in Table 4. The results are similar to those for the first case, except for the performance of EKF, UKF and MUKF for the real system. As explained in Section 4.2, all these three filters estimate the state to be 0 when their initial estimate is 0. However, numerical errors in the computation of the σ -points for MUKF result in divergence from 0. In any case, the strong dependence on the initial conditions of

Table 2 RMS estimation error and computation time for the example of Section 4.1, case II

Estim. technique	Mean x error	Mean y error	Max. x error	Max. y error	Comp. time (ms)
EKF	0.4899	1.4082	1.3000	116	0.15
UKF	0.3357	0.7314	0.7976	73.88	0.36
MUKF(P)	0.3357	0.7178	0.7950	71.50	0.61
MUKF	0.3336	0.8337	0.8042	92.05	0.77
UKF-mode	0.3379	0.3806	0.8273	0.864	0.55
MUKF-mode	0.3371	0.3868	0.8365	0.825	0.96
MUKF(15)-mode	0.3367	0.3843	0.8306	0.792	1.28
EKF-L	0.3916	0.4219	0.7965	0.865	0.72
UKF-L	0.3907	0.4199	0.7936	0.864	0.85
PF/SIR(50)	0.3413	0.3928/0.3969	0.8401	2.341/2.344	0.25
PF/SIR(1000)	0.3276	0.3594/0.3656	0.8037	1.273/1.272	1.80
CM(50)	0.3272	0.3607/0.3672	0.8112	1.007/1.017	0.08
CM(1000)	0.3271	0.3576/0.3641	0.8112	0.799/0.849	3.62

Table 3 RMS estimation error and computation time for the example of Section 4.2, case I

Estim. technique	(13), (16)			(19)–(20)		
	Mean error	Max error	Comp. time	Mean error	Max error	Comp. time
EKF	0.6879	2.1890	0.15	0.6524	0.9558	0.29
UKF	1.6435	3.8932	0.36	0.6525	0.9577	0.52
MUKF	1.1867	2.9310	0.29	0.6475	0.9655	0.46
PF/SIR(100)	0.6237	1.0864	0.28	0.6665	1.4922	0.42
PF/SIR(1000)	0.6136	0.9033	1.34	0.6566	1.2394	1.48
CM(30)	0.6331	1.4777	0.05	0.6370	0.9280	4.27
CM(100)	0.6137	0.9222	0.06	0.6368	0.9284	11.70

Table 4 RMS estimation error and computation time for the example of Section 4.2, case II

Estim. technique	(13), (16)			(19)–(20)		
	Mean error	Max error	Comp. time	Mean error	Max error	Comp. time
EKF	2.0468	4.8162	0.15	0.6518	0.9227	0.29
UKF	2.0468	4.8162	0.36	0.6519	0.9255	0.51
MUKF	1.9572	3.8193	0.29	0.6470	0.9321	0.45
PF/SIR(100)	0.6239	0.9027	0.28	0.6640	1.0056	0.42
PF/SIR(1000)	0.6150	0.8753	1.34	0.6550	0.9417	1.49
CM(30)	0.6324	1.2925	0.05	0.6365	0.8894	4.29
CM(100)	0.6147	0.8994	0.07	0.6363	0.8889	11.80

the results of these filters for the real system shows that it is better to apply them to the virtual system.

4.3 Two-dimensional bilinear system

The system studied in this subsection is described by the following equations

$$x_{k+1} = \begin{bmatrix} 0.5 & 0 \\ 0 & 0.5 \end{bmatrix} x_k + x_{1,k} x_{2,k} \begin{bmatrix} 0.25 \\ 0 \end{bmatrix} + w_k$$

$$y_k = [1 \quad 0] x_k + v_k$$

In the above equations, w_k and v_k are i.i.d. sequences of normal random variables, independent from each other and from the initial state which is also a normal random variable.

Since the output equation is linear, output inversion is not applicable, and the mode estimate described in Section 3.4 is identical to the estimated mean. Furthermore, the performance of PF/SIR was very bad even for 10 000 particles for which its computation time was very large. Thus, only the results for EKF, UKF and MUKF are presented. For MUKF, N was chosen to be equal to 2. Obviously, these three techniques differ only in the prediction step for this example, since the correction is accomplished using standard Kalman filtering equations. This, too, is possible because the output equation is linear.

For the first case studied, w_k is zero-mean and its covariance matrix is equal to $10I_2$, while v_k is zero-mean and its variance is 100. x_0 is also zero-mean with covariance matrix equal to $100I_2$. The system is simulated up to $k = 1000$. 1000 runs have been made. The RMS values of x_1 and x_2 are 40427 and 3.6578, respectively. The

results of the filtering techniques are presented in Table 5, while the corresponding values of the CRLB are 3.1966 and 3.1624. MUKF behaves clearly better than UKF, which is better than EKF. The difference is bigger for the maximum RMS error.

The second case differs in the variance of v_k which is now equal to 1000. 1000 runs are also made for this case, and for these runs, the RMS values for x_1 and x_2 are 10311 and 3.6518, respectively. Table 6 presents the corresponding filtering results. This time the difference between MUKF and UKF is much greater, especially in the worst-case performance. The CRLB values are now 3.3661 and 3.1624.

The results of this subsection show that under certain conditions, the proposed σ -point set can be used to get significantly better performance without an increase in computational cost.

4.4 Four-dimensional semi-realistic example

In the last subsection, a semi-realistic example of an armature controlled DC motor with a sin/cos encoder is studied. The field current is assumed constant and the magnetic non-linearities are neglected. θ denotes angular position, ω angular speed and i armature current. e is the voltage applied to the armature, used to control the motor, and for this example it will be assumed constant. The damping coefficient $b(t)$ is supposed to vary periodically. The system dynamics are given by (34)–(38).

$$\dot{\theta} = \omega \tag{34}$$

$$J\dot{\omega} = -b(t)\omega + Ki \tag{35}$$

$$L\dot{i} = e - K\omega - Ri \tag{36}$$

$$\dot{\phi}_b = \omega_{b0} \tag{37}$$

$$b(t) = b_0 + b_1 \cos(\phi_b) \tag{38}$$

The only quantity measured is the angular position, using a sin/cos encoder. It is assumed that measurements are taken every $\delta = 0.01$ s according to (39) and (40), where $v_{1,k}$ and $v_{2,k}$ are i.i.d. Gaussian random variables with zero-mean

and variance R_v .

$$y_{1,k} = \sin(\theta_k) + v_{1,k} \tag{39}$$

$$y_{2,k} = \cos(\theta_k) + v_{2,k} \tag{40}$$

In discrete time with time step equal to δ , and taking also into account that the system is subject to disturbance, the dynamics are approximated by the following equations

$$\theta_{k+1} = \theta_k + \delta\omega_k + w_{1,k} \tag{41}$$

$$\omega_{k+1} = \omega_k + \delta(-b_k\omega_k + Ki_k)/J + w_{2,k} \tag{42}$$

$$i_{k+1} = i_k + \delta(e - K\omega_k - Ri_k)/L + w_{3,k} \tag{43}$$

$$\phi_{b,k+1} = \phi_{b,k} + \delta\omega_{b0} + w_{4,k} \tag{44}$$

$$b_k = b_0 + b_1 \cos(\phi_{b,k}) \tag{45}$$

Thus, the problem is to estimate the state of the system with state (41)–(44), where b_k is defined by (45), and output (39) and (40).

As in Section 3.1, (39) and (40) can be inverted to provide a virtual measurement of θ , but in this case it is not so straightforward. It holds $\theta = \arctan(y_1 - v_1, y_2 - v_2)$, where $\arctan(y, x)$ is the angle whose sine and cosine are equal to $(y/\sqrt{x^2 + y^2})$ and $(x/\sqrt{x^2 + y^2})$, respectively. Let $R = \sqrt{y_1^2 + y_2^2}$, $\phi = \arctan(y_1, y_2)$ so that $y_1 = R \sin \phi$ and $y_2 = R \cos \phi$. Define the random variables $n = \cos\phi v_1 - \sin\phi v_2$ and $r = -\sin\phi v_1 - \cos\phi v_2$. They are jointly normally distributed and it can be verified through simple calculations that their variance is equal to R_v , as well as that they are uncorrelated and thus independent.

Let us define the random variable

$$q = -\frac{n}{r + R} \tag{46}$$

Table 5 RMS estimation error and computation time for the example of Section 4.3, case I

Estim. technique	Mean		Max		Comp. time
	x_1	x_2	x_1	x_2	
EKF	7.9181	3.5974	10.3128	3.9498	0.11
UKF	7.5795	3.5907	10.3435	3.9177	0.25
MUKF	6.6326	3.5734	7.9090	3.8778	0.29

Table 6 RMS estimation error and computation time for the example of Section 4.3, case II

Estim. technique	Mean		Max		Comp. time
	x_1	x_2	x_1	x_2	
EKF	33.2416	3.7100	69.4051	4.4110	0.11
UKF	29.0547	3.6893	73.0664	4.4738	0.25
MUKF	15.1896	3.6279	21.3721	3.9544	0.29

Then

$$\begin{aligned} \theta &= \arctan(R \sin \phi + r \sin \phi - n \cos \phi, R \cos \phi \\ &\quad + r \cos \phi + n \sin \phi) \\ &= \arctan((R+r) \sin \phi - n \cos \phi, (R+r) \cos \phi + n \sin \phi) \\ &= \arctan(\sin \phi + q \cos \phi, \cos \phi - q \sin \phi) \end{aligned} \quad (47)$$

Using the trigonometric identity

$$\tan(a+b) = \frac{\tan(a) + \tan(b)}{1 - \tan(a)\tan(b)} \quad (48)$$

the reader can check that

$$\begin{aligned} \theta &= \arctan(\sin \phi + q \cos \phi, \cos \phi - q \sin \phi) \\ &= \phi + \arctan(q) \end{aligned} \quad (49)$$

Since arctan is an odd function and the pdf of n is also odd, it follows that $\mathbb{E}[\arctan(q)] = 0$ thus $\mathbb{E}[\theta] = \phi$. The variance of $\arctan(q)$ depends on R .

It must be noted that ϕ is also the maximum likelihood estimator of θ . Indeed, the likelihood function is

$$\frac{1}{\sqrt{2\pi R_v}} e^{-((y_1 - \sin \phi)^2 / 2R_v)} \frac{1}{\sqrt{2\pi R_v}} e^{-((y_2 - \cos \phi)^2 / 2R_v)} \quad (50)$$

Thus it is maximised when the expression $(y_1 - \sin \phi)^2 + (y_2 - \cos \phi)^2$ is minimised. But

$$\begin{aligned} &(y_1 - \sin \phi)^2 + (y_2 - \cos \phi)^2 \\ &= y_1^2 + y_2^2 + \sin^2 \phi + \cos^2 \phi - 2(y_1 \sin \phi + y_2 \cos \phi) \\ &= y_1^2 + y_2^2 + 1 - 2(y_1 \sin \phi + y_2 \cos \phi) \end{aligned} \quad (51)$$

It is easy to verify that $(y_1 \sin \phi + y_2 \cos \phi)$ is maximised for $\phi = \arctan(y_1, y_2)$ and thus complete the argument.

A final remark is that the inversion gives $\theta \bmod 2\pi$. Thus to avoid 2π jumps at each time step, an integer multiple of 2π is added to $\arctan(y_1, y_2)$ so as to make the sum as close as possible to the previous estimated value of θ .

The system parameters for the simulations performed have been selected as follows (in SI units). $K = 0.035$, $L = 0.5$, $R = 2$, $J = 0.03$, $b_0 = 0.01$, $b_1 = 0.003$, $\omega_{b0} = 10$ and $e = 20$. The system is simulated up to time $t = 20$.

For the first case studied, the variance of w_k is equal to $10^{-4}I_4$, whereas the variances of $v_{1,k}$ and $v_{2,k}$ are equal to 10^{-4} . All noise sequences are normally distributed, i.i.d. and independent of each other and the initial condition

which follows the normal distribution with zero-mean and covariance matrix $0.01I_4$.

The results from 1000 runs are presented in Table 7. The values of the estimation error given are RMS values, while the RMS values for the four variables are equal to 298.6, 29.1, 9.4 and 115.5. The corresponding RMS values of the CRLB are 0.0079, 0.0909, 0.0364 and 0.1283.

For MUKF, N was chosen equal to 2. The results obtained using the mode were almost identical to those using the estimated mean; thus they are not included in the table. It must also be noted that for simplification the variance of q in (46), which depends on R , has been treated as constant, with value that for $R = 1$.

Except for PF, which cannot estimate ω and ϕ_b as accurately as the other methods, no differences between the filtering techniques can be observed. This happens because the filtering performance is close to the CRLB, so there is no room for improvement. This is verified by Figs. 6 and 7. In Fig. 6 the waveforms of the RMS value of the estimation error for the angular velocity as well as the corresponding Cramer–Rao bound are presented. The performance of KF-based methods is indeed very close to the CRLB. Fig. 7 presents the corresponding waveforms for the motor current and it can be observed that the values of the RMS error and the CRLB practically coincide. The reader can also observe that the RMS values follow the lower bound even during the transient. The RMS values for the estimates of θ also follow the lower bound, although the corresponding diagram is not presented for the sake of room. It must also be mentioned that the estimates of ϕ_b are not close to the CRLB (see also Fig. 8).

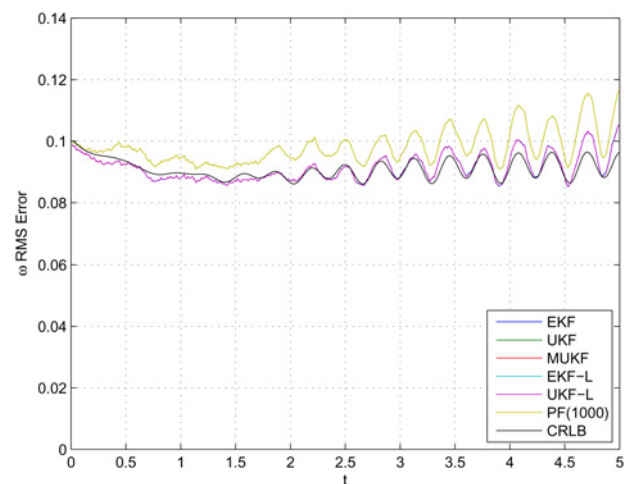


Fig. 6 Transient response of ω estimation error for various methods and CRLB, case I

Table 7 RMS estimation error and computation time for the example of Section 4.4, case I

Estim. technique	Mean				Max				Comp. time
	θ	ω	i	ϕ_b	θ	ω	i	ϕ_b	
EKF	0.0079	0.0968	0.0363	0.1942	0.0083	0.1384	0.0485	0.4230	0.16
UKF	0.0079	0.0967	0.0363	0.1942	0.0083	0.1384	0.0485	0.4235	0.57
MUKF	0.0079	0.0967	0.0363	0.1942	0.0083	0.1384	0.0485	0.4233	1.14
EKF-L	0.0079	0.0968	0.0363	0.1942	0.0084	0.1384	0.0485	0.4228	0.13
UKF-L	0.0079	0.0967	0.0363	0.1942	0.0084	0.1384	0.0485	0.4233	0.57
PF/SIR(1000)	0.0079	0.1077	0.0368	0.2492	0.0084	0.1793	0.0484	0.7624	1.59

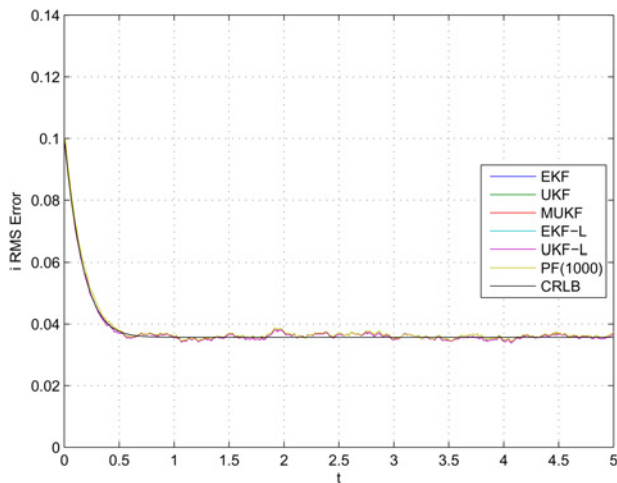


Fig. 7 Transient response of i estimation error for various methods and CRLB, case I

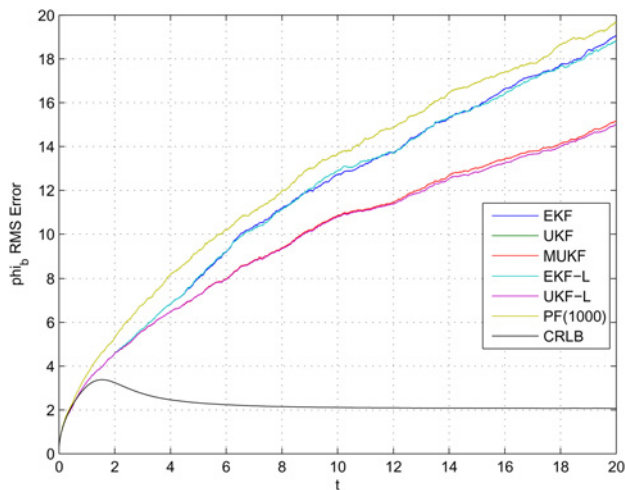


Fig. 8 Transient response of ϕ_b estimation error for various methods and CRLB, case II

The above system has been also studied with different noise and initial state covariances. Specifically, for the second case studied, the initial state covariance as well as the process noise is equal to $10^{-1}I_4$, whereas the variances of $v_{1,k}$ and $v_{2,k}$ are equal to 10^{-2} . The results from 1000 runs under these conditions are presented in Table 8. The RMS values for the four variables are equal to 300.8, 29.4, 9.5 and 115.6. This time there exist more significant differences between the performances of the various filtering algorithms. For example, while PF(1000) gives the best estimation for θ , it does not estimate ω very well. Output inversion also decreases the estimation error for θ as well as the error in the estimation of ω for EKF. UKF instead, which handles better non-linearities by its own, does not benefit from the inversion with respect to the estimation of ω .

As in the previous case, the CRLB practically coincides with the error of the best technique for i and θ , while it is close for ω . The diagrams are not presented for brevity. The diagram for ϕ_b , for which the divergence between CRLB and the values of estimation error is large, is presented in Fig. 8. The RMS values of the CRLB for the four state variables are equal to 0.0957, 2.6901, 1.1248 and 2.2860.

The computation times given are in milliseconds. MUKF is more demanding than UKF, but for this case both times are of the same order. This shows that MUKF can be used even for four-dimensional systems, at least with $N = 2$.

Under the noise characteristics of the second case, the mode estimate does not fully coincide with the mean estimate. Because the maximisation procedure, a subspace trust region method based on the interior-reflective Newton method described in [19, 20] and provided by the function ‘fminunc’ of MATLAB, is lengthy, only 100 runs have been made. The results are presented in Table 9. The reader may notice that the mode provides a better estimation of θ , on which the output depends. This is in accordance with the results of the previous examples.

Table 8 RMS estimation error and computation time for the example of Section 4.4, case II

Estim. technique	Mean				Max				Comp. time
	θ	ω	i	ϕ_b	θ	ω	i	ϕ_b	
EKF	0.1027	2.8636	1.1186	11.174	0.1084	4.2943	1.4269	39.3164	0.16
UKF	0.1017	2.7161	1.1184	9.2123	0.1066	4.1888	1.4208	32.3189	0.56
MUKF	0.1021	2.7176	1.1183	9.2943	0.1076	4.1978	1.4206	33.3555	1.12
EKF-L	0.1004	2.8578	1.1185	11.136	0.1050	4.2194	1.4279	48.5524	0.13
UKF-L	0.1004	2.7161	1.1184	9.2126	0.1050	4.1877	1.4207	32.3655	0.57
PF/SIR(1000)	0.0965	3.1289	1.1603	12.020	0.1012	4.9182	1.4557	47.6644	1.35

Table 9 Comparative results of mean and mode estimates for the example of Section 4.4, case II

Estim. technique	Mean				Max				Comp. time
	θ	ω	i	ϕ_b	θ	ω	i	ϕ_b	
MUKF	0.1021	2.7131	1.1261	9.3882	0.1060	3.5359	1.3459	24.1602	1.14
MUKF-mode	0.0960	2.7130	1.1261	9.3882	0.0991	3.5342	1.3459	24.1601	9.44

5 Conclusions

This paper shows that inverting the output equation to provide a virtual linear output can diminish non-linear phenomena and decrease the output estimation error. The output is also shown to be estimated very well using mode-based techniques in some cases. Using the dynamics of a specific function of the state instead of those of the state for estimation purposes has been also illustrated through an example, for which it leads to better performance of EKF and UKF. Finally, a new σ -point set for UKF is proposed and seems to significantly outperform the standard set in one example.

It was shown that the CRLB in some cases can be used to show that there is no room for improvement, whereas in some cases its value may be much lower than the lowest achievable value. Also, each of the proposed modifications helps in reducing the estimation error under certain conditions. To some extent, whether this will be the case or not can be expected according to the nature of the underlying problem. Some aspects of this subject have been reported in this paper.

Further research could address the general case for output equation inversion and estimating a specific function of the state. Since the cardinality of the proposed σ -point set increases exponentially with the dimension, it would be interesting to exploit sparsity patterns in the Jacobian of f in (1) or h in (2) to permit its application in high-order systems.

6 Acknowledgment

A preliminary version of this paper has been presented at the 17th Mediterranean Conference on Control and Automation, Thessaloniki, Greece, June 2009.

7 References

- 1 Kalman, R.E.: 'A new approach to linear filtering and prediction problem', *ASME J. Basic Eng.*, 1960, **82**, (1), pp. 35–45
- 2 Smith, G.L., Schmidt, S.F., McGee, L.A.: 'Application of statistical filter theory to the optimal estimation of position and velocity on board a circumlunar vehicle'. Technical Report TR R-135, NASA, 1962
- 3 Julier, S., Uhlmann, J.K.: 'Unscented filtering and nonlinear estimation', *Proc. IEEE*, 2004, **92**, (3), pp. 401–422
- 4 Sanjeev Arulampalam, M., Maskel, S., Gordon, N., Clapp, T.: 'A tutorial on particle filters for online nonlinear/non-Gaussian Bayesian tracking', *IEEE Trans. Signal Process.*, 2002, **50**, (2), pp. 174–188
- 5 Cappé, O., Godsill, S.J., Moulines, E.: 'An overview of existing methods and recent advances in sequential Monte Carlo', *Proc. IEEE*, 2007, **95**, (5), pp. 899–924
- 6 Lefebvre, T., Bruyninckx, H., Schutter, J.d.: 'Kalman filters for nonlinear systems: a comparison of performance', *Int. J. Control*, 2004, **77**, (7), pp. 639–653
- 7 Julier, S., Uhlmann, J.K., Durrant-Whyte, H.F.: 'A new method for the nonlinear transformation of means and covariances in filters and estimators', *IEEE Trans. Autom. Control*, 2000, **45**, (3), pp. 477–482
- 8 Bayes, T.: 'An essay towards solving a problem in the doctrine of chances', *Phil. Trans. R. Soc. London*, 1763, **53**, pp. 370–418
- 9 Billingsley, P.: 'Probability and measure' (Wiley-Interscience, Hoboken, NJ, 1995, 3rd edn.)
- 10 Crisan, D., Doucet, A.: 'A survey of convergence results on particle filtering methods for practitioners', *IEEE Trans. Signal Process.*, 2002, **50**, (3), pp. 736–746
- 11 Hu, X.-L., Schon, T.B., Ljung, L.: 'A basic convergence result for particle filtering', *IEEE Trans. Signal Process.*, 2008, **56**, (4), pp. 1337–1348
- 12 van der Merwe, R., Doucet, A., de Freitas, N., Wan, E.: 'The unscented particle filter'. INFENF/TR 380, Cambridge University, August 2000
- 13 Gordon, N.J., Salmond, D.J., Smith, A.F.M.: 'Novel approach to nonlinear/non-Gaussian state estimation', *IEE Proc.-F*, 1993, **140**, (2), pp. 107–113
- 14 Kitagawa, G.: 'Monte Carlo filter and smoother for non-Gaussian nonlinear state space models', *J. Comput. Graph. Stat.*, 1996, **5**, (1), pp. 1–25
- 15 Cramer, H.: 'Mathematical methods of statistics' (Princeton University Press, Princeton, NJ, 1946)
- 16 Rao, C.: 'Information and the accuracy attainable in the estimation of statistical parameters', *Bull. Calcutta Math. Soc.*, 1945, **37**, pp. 81–89
- 17 van Trees, H.L.: 'Detection, estimation and modulation theory' (Wiley, New York, 1968)
- 18 Tichavsky, P., Muravchik, C.H., Nehorai, A.: 'Posterior Cramer–Rao bounds for discrete-time nonlinear filtering', *IEEE Trans. Signal Process.*, 1998, **46**, (5), pp. 1386–1396
- 19 Coleman, T.F., Li, Y.: 'An interior, trust region approach for nonlinear minimization subject to bounds', *SIAM J. Optim.*, 1996, **6**, pp. 418–445
- 20 Coleman, T.F., Li, Y.: 'On the convergence of reflective newton methods for large-scale nonlinear minimization subject to bounds', *Math. Program.*, 1994, **67**, (2), pp. 189–224